

Hopf Bifurcation and Sliding Mode Control of Chaotic Vibrations in a Four-dimensional Hyperchaotic System

Wen-ju Du, Jian-gang Zhang and Shuang Qin

Abstract—The basic dynamic properties of a four dimensional hyperchaotic system are investigated in this paper. More precisely, the stability of equilibrium point of hyperchaotic system is studied by means of nonlinear dynamics theory. We analyse the existence and stability of Hopf bifurcation, and the formulas for determining the direction of Hopf bifurcation and the stability of bifurcating periodic solutions are derived. In addition, a sliding mode controller is designed and controlled the hyperchaotic system to any fixed point to eliminate the chaotic vibration by means of sliding mode method. Finally, the numerical simulations were presented to confirm the effectiveness of the controller.

Index Terms—Stability, Lyapunov exponents, Hopf bifurcation, Sliding mode control

I. INTRODUCTION

The discovery of the eminent Lorenz system [1] has led to an extensive study of chaotic behaviors in nonlinear systems due to many possible applications in science and technology. There is a huge volume of literature devoted to the study of the nonlinear characteristics and basic dynamic properties of chaotic system [2]. And the nonlinear dynamics and chaos theory has been in-depth researched during the last decades [3]. Despite the simplicity of four-dimensional autonomous systems, these systems have a rich dynamical behavior, ranging from stable equilibrium points to periodic and even chaotic oscillations, depending on the parameter values. Moreover, the research and application on bifurcation of autonomous systems has become a very popular topic [4-9]. Over the past few decades, more and more chaotic phenomena have been found in many research fields and it can be widely used in secure communication, information processing, nonlinear circuits, biological systems, and chemical reactions. Many scholars paid great effort to generate chaos and analyze its dynamic characteristics. Dias and Mello [10] studied the

nonlinear dynamics of a Lorenz-like system. Sotomayor et al. [11] used the projection method described in [12] to calculation of the first and second Lyapunov coefficients associated to Hopf bifurcations of the Watt governor system, and it was extended to the calculation of the third and fourth Lyapunov coefficients. Zhang et al. [13] presented a new three-dimensional autonomous chaotic system and investigated its basic dynamic properties via theoretical analysis and numerical simulation. Jana et al. [14] studied the stability and Hopf bifurcation for a harvested predator-prey system which incorporates feedback delay in prey growth rate.

In recent years, the research of robust control system has made considerable progress and development in theory and practical application. As a representative of the nonlinear robust control theory, variable structure control theory has been widely researched around the world, and also has an increasing number of industrial applications. Lee et al. [15] presented a sliding-mode controller with integral compensation for a magnetic suspension balance beam system, and the control scheme comprises an integral controller which is designed for achieving zero steady-state error under step disturbances. Takuro et al. [16] applied the sliding mode control to achieve the robust control of space robot in capturing operation of the target and controlling the spacecraft motion under unknown parameters, like mass and inertia tensor. Chen et al. [17] proposed a no-chattering sliding mode control strategy for a class of fractional-order chaotic systems, and the designed control scheme guarantees the asymptotical stability of an uncertain fractional-order chaotic system. To ensure the robustness of the system control, Chen et al. stabilized the chaotic orbits to arbitrary chosen fixed points and periodic orbits by means of sliding mode method and they presented numerical simulations to confirm the validity of the controller [18]. Chen et al. [19] eliminated the chaotic vibration of hydro-turbine governing system by using the sliding mode method, and controlled the system to any fixed point and any periodic orbit. In this paper, we consider a novel four-dimensional hyperchaotic system which proposed by Gao [20]. He just analyzed the stability of equilibrium, such as the phase diagram of attractors, the bifurcation diagram and Lyapunov exponent. However, the Hopf bifurcation and chaos control of the four-dimensional hyperchaotic system has not been clarified yet. So, in this paper we investigate the bifurcations and sliding mode control of chaotic vibrations of the novel four-dimensional hyperchaotic system.

The rest of this paper is organized as follows. In section 2, the description of the model is presented. The linear analysis of equilibria and the existence of Hopf bifurcation at equilibrium are investigated in section 3. In section 4, we

Manuscript received October 3, 2015; revised December 6, 2015. This work is supported by the National Natural Science Foundation (No.11161027, No.61364001).

Wen-ju Du is with the School of Traffic and Transportation, Lanzhou Jiaotong University, Lanzhou, China (phone: 086-9314956002; fax: 086-9314956002; e-mail: duwenjuok@126.com).

Jian-gang Zhang, Shuang Qin was with Department of Mathematics, Lanzhou Jiaotong University, Lanzhou, China (e-mail: zhangjg7715776@126.com, qinshuangok@126.com).

analyzed the direction of Hopf bifurcation and the stability of bifurcating periodic solutions. The numerical simulations are given to illustrate the theoretical analysis in section 5. And in section 6, we controlled the system to any fixed point and any periodic orbit to eliminate the chaotic vibration by means of sliding mode method. Section 7 concludes the paper.

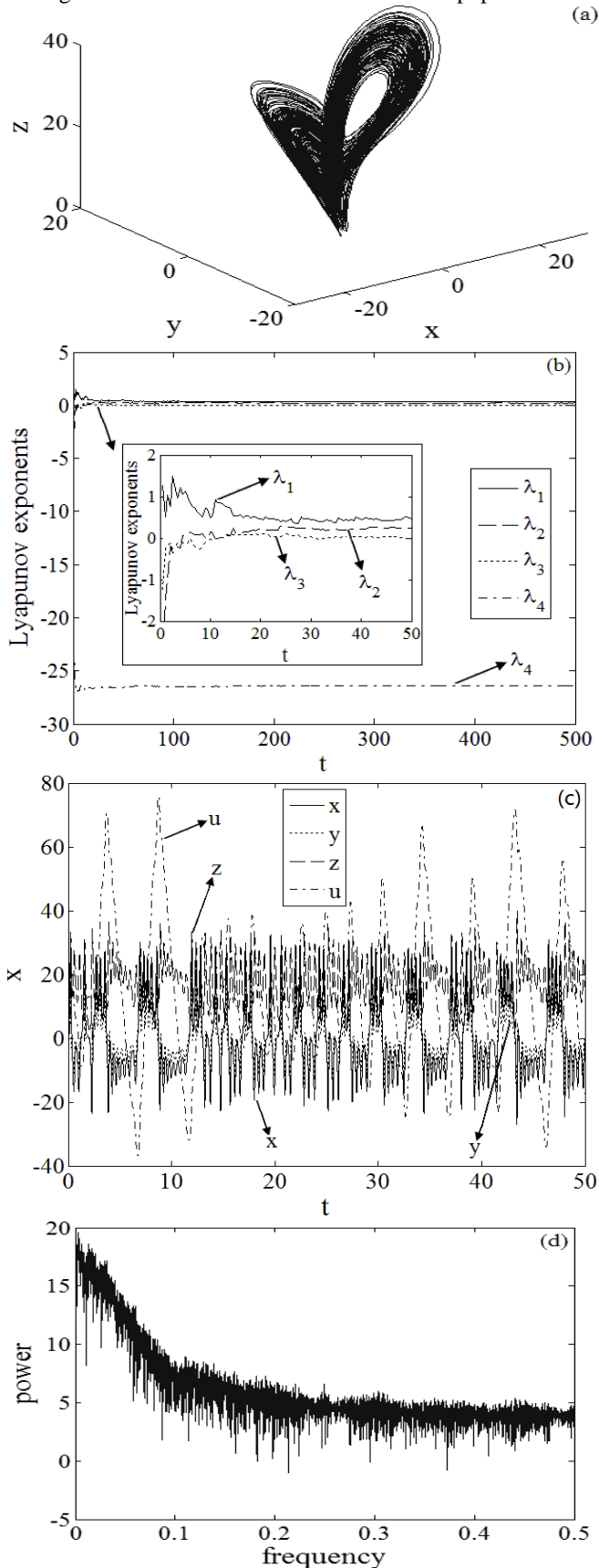


Fig. 1. (a)Phase trajectory in 3-D space, (b)Lyapunov-exponent spectrum, (c)Time history, (d) Frequency spectrum.

II. DESCRIPTION OF THE MODEL

In this paper, we investigate a four-dimensional hyperchaotic system as follows:

$$\begin{cases} \dot{x} = -ax + by, \\ \dot{y} = ax - xz - y - u, \\ \dot{z} = xy - c(x + z), \\ \dot{u} = mx, \end{cases} \quad (1)$$

where $(x, y, z, u) \in R^4$ are state variables, a, b, c, m are real constants. The system (1) has a hyperchaotic attractor when the real constants $a = 20, b = 35, c = 5, m = 4$, as show in Fig. 1 (a). Moreover, the dynamics of the system (1) can be characterized with its Lyapunov exponents which are computed numerically by Wolf algorithm proposed in [21], where the Lyapunov exponents: $\lambda_1=0.3477, \lambda_2=0.1983, \lambda_3=0, \lambda_4=-26.4303$, as show in Fig. 1 (b), and the Lyapunov dimension $D_{KY}=3.02065$. Fig. 1 (c) and Fig. 1 (d) shows the time history and frequency spectrum of hyperchaotic attractor, respectively.

III. STABILITY ANALYSIS

In this section, we study the stability of equilibrium and the existence of Hopf bifurcation. In a vectorial notation which will be useful in the calculations, system (1) can be written as $x' = f(x, \zeta)$, where

$$x' = f(x, \zeta) = (-ax + by, ax - xz - y - u, xy - c(x + z), mx), \quad (2)$$

$x = (x, y, z, u) \in R^4$ and $\zeta = (a, b, c, d) \in R^4$.

By solving the following equations simultaneously $-ax + by = 0, ax - xz - y - u = 0, xy - c(x + z) = 0, mx = 0$, (3) we get the system has a unique equilibrium $E_0 = (0, 0, 0, 0)$.

Lemma 1. The polynomial $L(\lambda) = \lambda^3 + p_1\lambda^2 + p_2\lambda + p_3$ with real coefficients has all roots with negative real parts if and only if the numbers p_1, p_2, p_3 are positive and the inequality $p_1 p_2 > p_3$ is satisfied.

We have the following proposition.

Proposition 1. The equilibrium E_0 is unstable if $m > m_0$. If $a > -1, mb > 0, a(1-b) > 0, c > 0$ and

$$m < m_0 = \frac{a(a+1)(1-b)}{b}, \quad (4)$$

then the equilibrium E_0 is asymptotically stable.

Proof. The Jacobian matrix at the fixed point E_0 is given by

$$A = \begin{pmatrix} -a & b & 0 & 0 \\ a & -1 & 0 & -1 \\ -c & 0 & -c & 0 \\ m & 0 & 0 & 0 \end{pmatrix}, \quad (5)$$

and its characteristic polynomial is

$$p(\lambda) = (\lambda + c)[\lambda^3 + (a+1)\lambda^2 + (a-ab)\lambda + mb], \quad (6)$$

According to Lemma 1, the equilibrium E_0 is unstable if $m > m_0$. And if the real parts of all the roots λ of equation (6) are negative if and only if

$$c > 0, a > -1, mb > 0, a(1-b) > 0, m < m_0,$$

So the proposition follows.

Proposition 2. Assume that $a > 0, b < 0, c > 0$. If equation (6) has a pair of purely imaginary roots $\lambda_{1,2} = \pm i\omega_0$ and $\text{Re}(\lambda'_m(m_0)) \neq 0$, then the Hopf bifurcation occurs at the point E_0 when the bifurcation parameter m pass through the critical value m_0 .

Proof. Let $\lambda = i\omega(\omega > 0)$ is a root of Eq. (6), we have

$$-i\omega^3 - (a+1)\omega^2 + (a-ab)i\omega + mb = 0, \tag{7}$$

then separating the real and imaginary parts of equation (7), and we get

$$\begin{cases} -\omega^3 + (a-ab)\omega = 0, \\ -(a+a)\omega^2 + mb = 0. \end{cases} \tag{8}$$

Through calculation, we have

$$\omega = \omega_0 = \sqrt{a-ab}, m = m_0 = \frac{a(a+1)(1-b)}{b}, \tag{9}$$

and the following four characteristic roots

$$\lambda_{1,2} = \pm i\omega_0, \lambda_3 = -c, \lambda_4 = -(a+c), \tag{10}$$

Take the derivative of both sides of Eq. (6) with respect to m , we obtain

$$\frac{d\lambda}{dm} = -\frac{b}{3\lambda^2 + 2(a+1)\lambda + (a-ab)}, \tag{11}$$

and

$$\begin{aligned} \left. \frac{d \text{Re} \lambda}{dm} \right|_{m=m_0} &= \frac{b}{2(2a-ab+1)} < 0, \\ \left. \frac{d \text{Im} \lambda}{dm} \right|_{m=m_0} &= \frac{a+1}{2(2a-ab+1)} > 0. \end{aligned} \tag{12}$$

Assume that $a > 0, b < 0, c > 0$, when m passes through the critical value m_0 , the system(1) occurs Hopf bifurcation at the equilibrium $E_0 = (0, 0, 0, 0)$.

IV. HOPF BIFURCATION ANALYSIS

In this section, we study the direction and stability of Hopf bifurcation under the condition $a > 0, b < 0, c > 0$ and $m = m_0$.

Using the notion described in [10], the multilinear symmetric functions corresponding to f can be written as

$$\begin{aligned} B(x, y) &= (0, -x_1y_3 - x_3y_1, x_1y_2 + x_2y_1, 0)^T, \\ C(x, y, z) &= (0, 0, 0, 0)^T, \end{aligned} \tag{13}$$

The eigenvalues of A are

$$\lambda_{1,2} = \pm i\omega_0, \lambda_3 = -c, \lambda_4 = -(a+c), \tag{14}$$

Let $p, q \in C^4$ be vectors such that

$$Aq = i\omega_0q, A^T p = -i\omega_0p, \langle p, q \rangle = \sum_{i=1}^4 \bar{p}_i q_i = 1, \tag{15}$$

where A^T is the transpose of the matrix A , and by calculate we get

$$\begin{aligned} q &= \left(\frac{\omega_0 i}{m}, \frac{-\omega_0^2 + a\omega_0 i}{bm}, \frac{-c\omega_0^2 - c^2\omega_0 i}{m(c^2 + \omega_0^2)}, 0 \right)^T \\ p &= \left(\frac{m\omega_0(a+1) + m(a+1+2\omega_0^2)i}{\omega_0(a+1)^2 + 4\omega_0^3}, \frac{-2bm\omega_0 + bm(a+1)i}{\omega_0(a+1)^2 + 4\omega_0^3}, \right. \\ &\quad \left. 0, \frac{bm(a+1) + 2bm\omega_0 i}{\omega_0^2(a+1)^2 + 4\omega_0^4} \right)^T \end{aligned} \tag{16}$$

$$B(q, q) = \left(0, \frac{-2c^2\omega_0^2 + 2c\omega_0^3 i}{m^2(c^2 + \omega_0^2)}, \frac{-2\omega_0^2(a + \omega_0 i)}{bm^2}, 0 \right)^T, \tag{17}$$

$$B(q, \bar{q}) = \left(0, \frac{-2c^2\omega_0^2}{m^2(c^2 + \omega_0^2)}, \frac{2\omega_0^2 a}{bm^2}, 0 \right)^T, \tag{18}$$

$$h_{11} = \left(0, 0, \frac{-2\omega_0^2 a}{bcm^2}, \frac{-2c^2\omega_0^2}{m^2(c^2 + \omega_0^2)} \right)^T, \tag{19}$$

$$\begin{aligned} h_{20} &= (2i\omega_0 E_3 - A)^{-1} B(q, q) \\ &= (h_1 + h_2 i, h_3 + h_4 i, h_5 + h_6 i, h_7)^T, \end{aligned} \tag{20}$$

where

$$\begin{aligned} h_1 &= \frac{k_1 k_3 + k_2 k_4}{k_3^2 + k_4^2}, h_2 = \frac{k_2 k_3 - k_1 k_4}{k_3^2 + k_4^2}, h_3 = \frac{k_5}{k_7}, h_4 = \frac{k_6}{k_7}, \\ h_5 &= \frac{-2\omega_0^2(k_3 k_8 + k_4 k_9)}{bm^2(c^2 + 4\omega_0^2)(k_3^2 + k_4^2)}, h_6 = \frac{-2\omega_0^2(k_3 k_9 - k_4 k_8)}{bm^2(c^2 + 4\omega_0^2)(k_3^2 + k_4^2)}, \\ h_7 &= \frac{b(2\omega_0^3 i - 2c^2\omega_0^2)}{2m(c^2 + \omega_0^2)(2a\omega_0^2 - a\omega_0 i - bm/2 + 2\omega_0^2 + 4\omega_0^3 i + ab\omega_0 i)}, \\ k_1 &= 2bc\omega_0^4(2c-1)(4\omega_0^2 + ab-a) - 4b\omega_0^4(c^3 + 2\omega_0^2), \\ k_2 &= 2b\omega_0^3(c^3 + 2\omega_0^2)(a-4\omega_0^2 - ab) - 4b\omega_0^5(2c-1)(a+1), \\ k_3 &= -m^2(c^2 + \omega_0^2)(r_1 r_2 + r_3 r_4), k_5 = 8\omega_0(r_5 r_7 - r_6 r_8), \\ k_4 &= -m^2(c^2 + \omega_0^2)(r_1 r_4 + r_2 r_3), k_6 = 8\omega_0(r_5 r_8 + r_6 r_7), \\ k_7 &= m^2(c^2 + \omega_0^2)(4a^2 b^2 \omega_0^2 - 8a^2 b \omega_0^2 + 16a^2 \omega_0^4 + 4a^2 \omega_0^2 \\ &\quad - 8abm\omega_0^2 + 32ab\omega_0^4 + b^2 m^2 - 8bm\omega_0^2 + 64\omega_0^6 + 16\omega_0^4), \\ k_8 &= r_9(ac + \omega_0^2) + r_{10}\omega_0(c-2a), k_9 = r_{10}(ac + \omega_0^2) + r_9\omega_0(c-2a), \\ r_1 &= 2a\omega_0^2 - ab/2 + 2\omega_0^2, r_2 = 4\omega_0^2(a+1) + c(ab-a+4\omega_0^2), \\ r_3 &= 4\omega_0^3 - ab\omega_0 - a\omega_0, r_4 = 2c\omega_0(a+1) - 2\omega_0(ab-a+4\omega_0^2), \\ r_5 &= 2\omega_0^2(ac^2 + \omega_0^2), r_7 = 2\omega_0^3 - a\omega_0/2 + ab\omega_0/2, \\ r_6 &= 2\omega_0^3(2c^2 - a), r_9 = 4bc^3\omega_0^4 - 2bc\omega_0^4(a-ab-4\omega_0^2), \\ r_8 &= \omega_0^2 + a\omega_0^2 - bm/4, r_{10} = 2bc^3\omega_0^3(4\omega_0^2 + ab-a) - 4bc\omega_0^5(a+1), \end{aligned}$$

Through direct calculation, we also has

$$B(q, h_{11}) = (0, \frac{2a\omega_0^3 i}{bcm^3}, 0, 0)^T, \tag{21}$$

$$B(\bar{q}, h_{20}) = (0, n_1 + n_2 i, n_3 + n_4 i, 0)^T,$$

$$H_{21} = (0, n_1 + (n_2 + \frac{4a\omega_0^3}{bcm^3})i, n_3 + n_4 i, 0)^T, \tag{22}$$

$$\begin{aligned} G_{21} &= \frac{bm}{\omega_0(a+1)^2 + 4\omega_0^3} \left[(a+1)(n_2 + \frac{4a\omega_0^3}{bcm^3}) - 2\omega_0 n_1 \right] - \\ &\quad \frac{bm}{\omega_0(a+1)^2 + 4\omega_0^3} \left[n_1(a+1) - 2\omega_0(n_2 + \frac{4a\omega_0^3}{bcm^3}) \right] i, \end{aligned} \tag{23}$$

where

$$\begin{aligned} n_1 &= \frac{h_1 c \omega_0^2 + h_2 c^2 \omega_0 - h_6 \omega_0 (c^2 + \omega_0^2)}{m(c^2 + \omega_0^2)}, n_3 = \frac{h_4 b \omega_0 - h_1 \omega_0^2 + h_2 a \omega_0}{bm}, \\ n_2 &= \frac{h_2 c \omega_0^2 - h_1 c^2 \omega_0 + h_5 \omega_0 (c^2 + \omega_0^2)}{m(c^2 + \omega_0^2)}, n_4 = \frac{-h_3 b \omega_0 - h_4 a \omega_0 + h_2 \omega_0^2}{bm}. \end{aligned}$$

Theorem 1. Consider the four-parameter family of differential equations (1). The first Lyapunov coefficient associated to the equilibrium E_0 is given by

$$l_1(a, b, c) = \frac{(a+1)(bcm^3 n_2 + 4a\omega_0^3) - 2bcm^3 \omega_0 n_1}{2bcm^2 \omega_0 [(a+1)^2 + 4\omega_0^2]}. \tag{24}$$

If l_1 is different from zero, then system (1) has a transversal Hopf point at E_0 .

V. NUMERICAL EXAMPLE

Next, we give a numerical example of Hopf bifurcation. Let $a=2, b=-1$, and by compute we get the critical value $m_0 = -12$. The equilibrium is stable when $m = -10 > m_0$ and unstable when $m = -14 < m_0$, as show in Fig. 2. From the formulas in previous section, we have $l_1 = -0.362681 < 0$. Thus, the periodic solution bifurcating from E_0 is supercritical and stable.

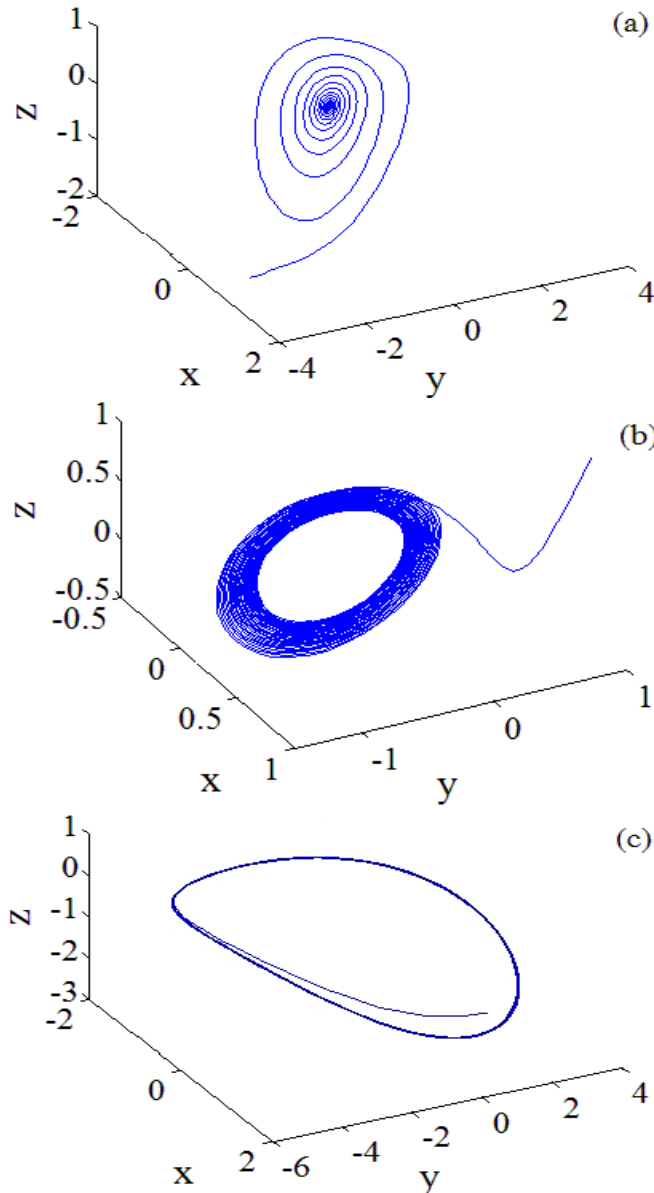


Fig. 2. Phase diagram of system (1) with (a) $a=2, b=-1, c=5, m=-10$, (b) $a=2, b=-1, c=5, m=-12$, (c) $a=2, b=-1, c=5, m=-14$.

The bifurcation phenomenon can be detected by examining graphs of x versus the control parameter m for system (1). We fixed $a=20, b=35, c=5$ and while m varies on the interval $[50, 70]$, the bifurcation diagrams and corresponding Lyapunov exponent spectrum, as show in Fig. 3. Obviously, with the increase of the parameter m , the system is undergoing some representative dynamical routes, such as chaos, period-doubling bifurcations and periodic loops.

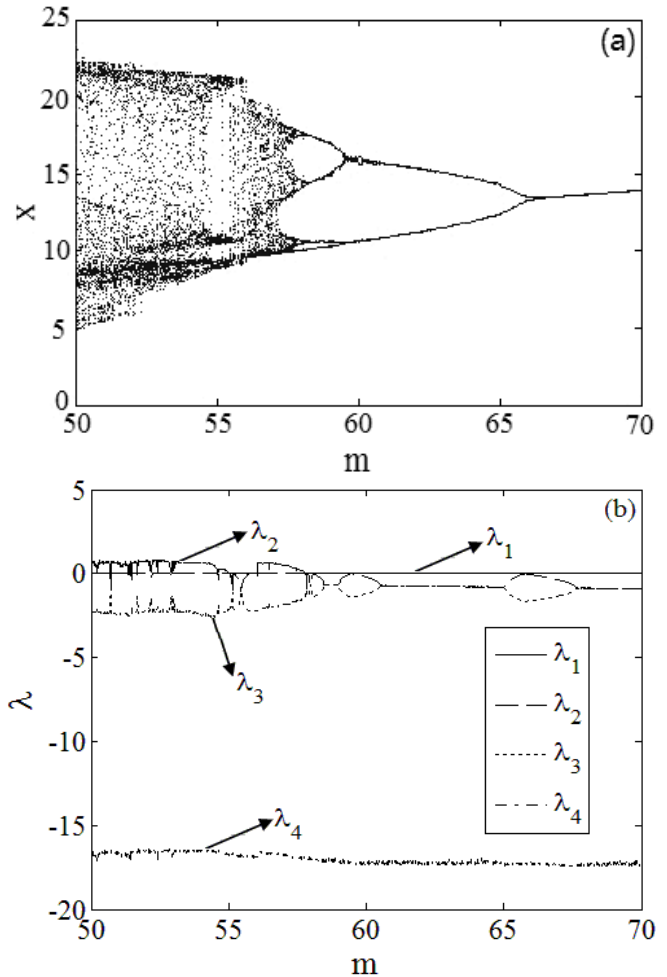


Fig. 3. Nonlinear dynamics of system (1) for specific values $a=20, b=35, c=5$ versus the control parameter m (a) bifurcation diagram of x ; (b) Lyapunov exponent spectrum.

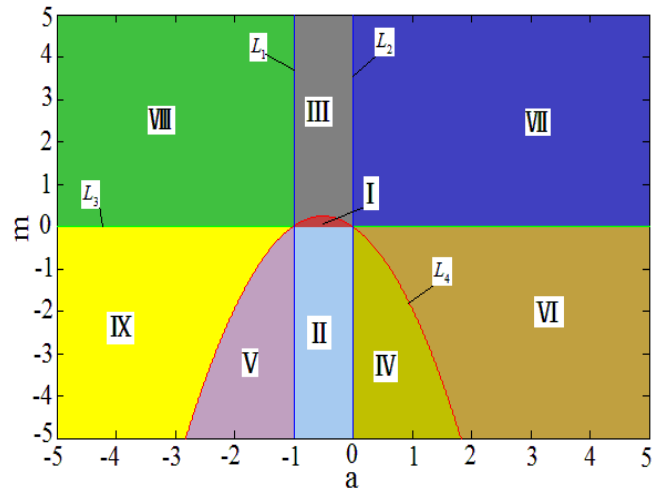


Fig. 4. The stable region on the parameter plane (a, m) .

Fixed the parameters $b=35, c=5$, and we can get the characteristic polynomial of the Jacobian matrix of system (1) at E_0 is

$$p(\lambda) = (\lambda + 5)[\lambda^3 + (a + 1)\lambda^2 - 34a\lambda + 35m], \quad (25)$$

the equilibrium E_0 is asymptotically stable if $-1 < a < 0, m > 0, -34a(a + 1) > 35m$ and the system (1) has a transversal Hopf point at E_0 if $-1 < a < 0, m > 0, -34a(a + 1) = 35m$. Let $a + 1 = 0, -34a = 0, 35m = 0, -34a(a + 1) - 35m = 0$, and draw the stability region on the parameter plane $a - m$, as show

in Fig. 4. In the figure, the symbol $L_i, i=1,2,3,4$ represents $a+1=0, -34a=0, 35m=0$ and $-34a(a+1)-35m=0$, respectively. The Hopf bifurcation conditions are satisfied on the curve L_4 . In region (I), we have $m > 0, -34a(a+1) > 35m$ $-1 < a < 0$, and all points are stable, but in other regions the points are unstable.

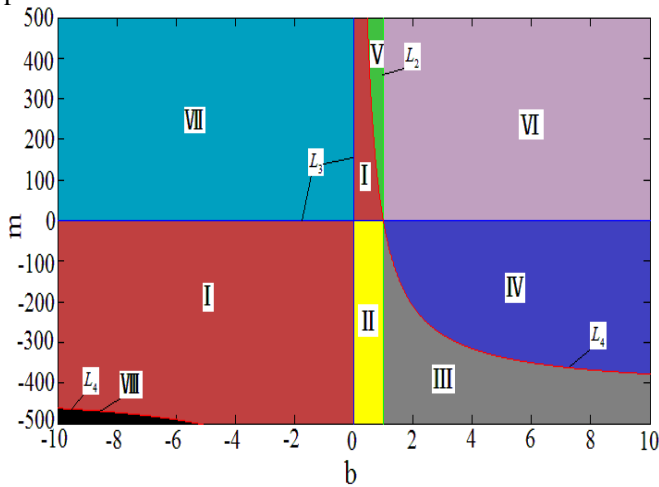


Fig. 5. The stable region on the parameter plane (b, m) .

Fixed the parameters $a = 20, c = 5$, and the characteristic polynomial of the Jacobian matrix of system (1) at E_0 is

$$p(\lambda) = (\lambda + 5)[\lambda^3 + 21\lambda^2 + 20(1 - b)\lambda + mb], \quad (26)$$

the equilibrium E_0 is asymptotically stable if $b < 1, mb > 0, 420(1 - b) > mb$, and the system (1) has a transversal Hopf point at E_0 if $b < 1, mb > 0, 420(1 - b) = mb$. Let $b = 1, mb = 0, 420(1 - b) - mb = 0$, and use MATLAB to draw the stability region on the parameter plane $b-m$, as show in Fig. 5. The symbol $L_i, i = 2, 3, 4$ represents $b = 1, mb = 0$ and $420(1 - b) - mb = 0$. The Hopf bifurcation conditions are satisfied on the curve L_4 . In region (I), we have $b < 1, mb > 0, 420(1 - b) > mb$ and all points are stable, but in other regions the points are unstable.

VI. SLIDING MODE CONTROL OF CHAOTIC VIBRATIONS

6.1 The design of the controller

We designed a sliding surface with good nature and made the system possess the desired properties when make the system limits on the sliding surface. In order to facilitate control, we make the system reach the sliding surface and keep sliding. After joining the controller, the system (1) has the following form

$$\begin{cases} \dot{x} = -20x + 35y + d_1 + u_1, \\ \dot{y} = 20x - xz - y - u + d_2 + u_2, \\ \dot{z} = xy - 5(x + z) + d_3 + u_3, \\ \dot{u} = 4x + d_4 + u_4. \end{cases} \quad (27)$$

where u_1, u_2, u_3 and u_4 are control inputs. We can control the chaos to the required range or a fixed point if we join a reasonable controller.

Defined the following matrix

$$A = \begin{pmatrix} -20 & 35 & 0 & 0 \\ 20 & -1 & 0 & -1 \\ -5 & 0 & -5 & 0 \\ 4 & 0 & 0 & 0 \end{pmatrix}, \quad B = \begin{pmatrix} 1 & 0 & 0 & 0 \\ 0 & 1 & 0 & 0 \\ 0 & 0 & 1 & 0 \\ 0 & 0 & 0 & 1 \end{pmatrix},$$

$$d = \begin{pmatrix} d_1 \\ d_2 \\ d_3 \\ d_4 \end{pmatrix}, \quad g = \begin{pmatrix} 0 \\ -xz \\ xy \\ 0 \end{pmatrix},$$

where A is the linear matrix of the system, B is the control matrix, d is the bounded perturbation matrix, and g is the nonlinear matrix of the system. The control goal is to let the system's state $x = [x_1, x_2, x_3, x_4]^T$ tracking a time-varying state $x_d = [x_{d1}, x_{d2}, x_{d3}, x_{d4}]^T$. So, we can define the following tracking error

$$e = x - x_d, \quad (28)$$

The error system can be written as

$$\dot{e} = \dot{x} - \dot{x}_d = Ax + Bg + Bu + d - \dot{x}_d, \quad (29)$$

Define a time-varying proportional integral sliding mode surface

$$S = Ke - \int_0^t K(A - BL)e(\tau) d\tau, \quad (30)$$

where $K \in R^{4 \times 4}, \det(KB) \neq 0$. To facilitate the calculation, we let $K = \text{diag}(1, 1, 1, 1)$. The additional matrix $L \in R^{4 \times 4}$, and $A - BL$ is negative definite matrix. Under the sliding mode, the equation $S = \dot{S} = 0$ must be satisfied, where

$$\dot{S} = KBg + KBLE + KBu + Kd + KAx_d - K\dot{x}_d, \quad (31)$$

To meet the sliding conditions, the following controller is designed

$$u = -[g + Le] - (KB)^{-1} [KAx_d - K\dot{x}_d] - (KB)^{-1} [\varepsilon + \|KBg\|] \text{sign}(S), \quad (32)$$

where $\text{sign}(S)$ is sign function.

Proposition 3.^[17] Assume that the constant ε satisfied the inequality $\varepsilon > \delta_1 + \delta_2 + 1$, where δ_1, δ_2 are arbitrary small positive numbers. Then the system (27) can reach the sliding mode $S = 0$ in a limited time under the controller (32), and the state variables and the selected reference state x_d are identical.

Proof. Construct the Lyapunov function $V = S^T S = \sum_{i=1}^4 S_i^2$,

according to (30), (31) and (32) one has

$$\begin{aligned} S^T \dot{S} &= S^T (KBg + KBLE + KBu + Kd + KAx_d - K\dot{x}_d) \\ &= S^T [Kd - (\varepsilon + \|KBg\|) \text{sign}(S)] \\ &\leq S^T [d - \varepsilon \text{sign}(S)] \\ &\leq \sum_{i=1}^4 |S_i| \delta_1 + \sum_{i=1}^4 |S_i| \delta_2 - \sum_{i=1}^4 |S_i| \varepsilon \\ &= |\delta_1 + \delta_2 - \varepsilon| \sum_{i=1}^4 |S_i| < -\sum_{i=1}^4 |S_i|. \end{aligned}$$

By the same token, we get

$$\dot{S}^T S < -\sum_{i=1}^4 |S_i|, \quad \dot{V} = \dot{S}^T S + S^T \dot{S} < -2 \sum_{i=1}^4 |S_i|.$$

So the proposition follows.

6.2 The numerical simulation

In the case of $u_1 = u_2 = u_3 = u_4 = 0$, the time-domain charts of the state variables of system (27) as show in Fig. 6. Fig. 6 illustrates that the system (27) has an aperiodic motion state before control.

In order to control the system (27) to the target state, we select the eigenvalue of $A - BL$ are $P = [-5, -5, -5, -5]$. The pole-placement method is adopted to get the following matrix

$$L = \begin{pmatrix} -15 & 35 & 0 & 0 \\ 20 & 4 & 0 & -1 \\ -5 & 0 & 0 & 0 \\ 4 & 0 & 0 & 5 \end{pmatrix}. \quad (33)$$

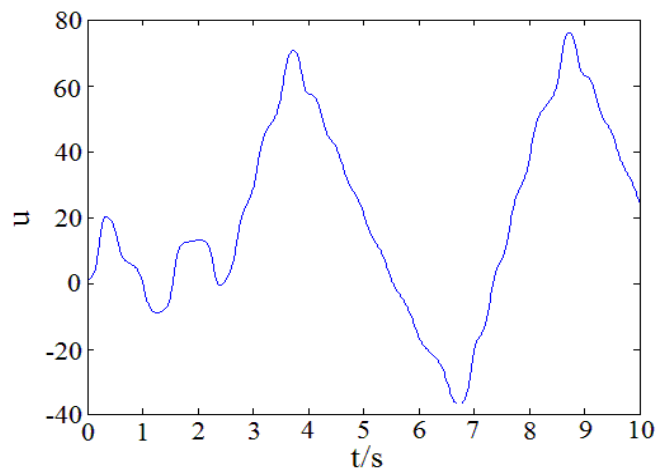
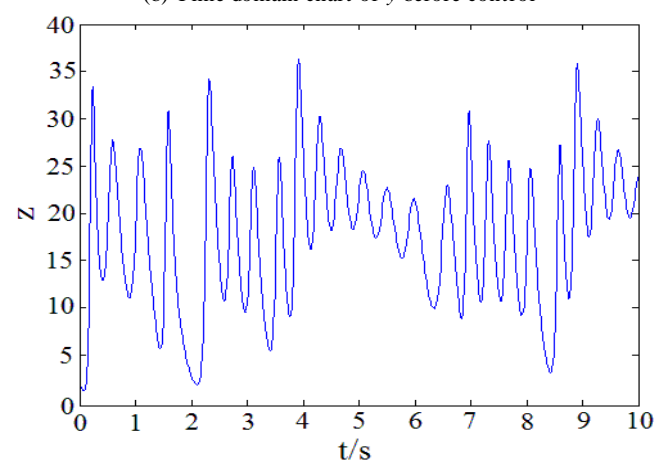
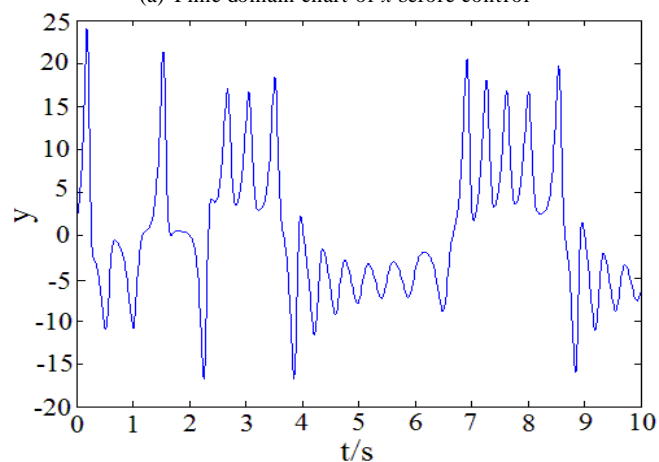
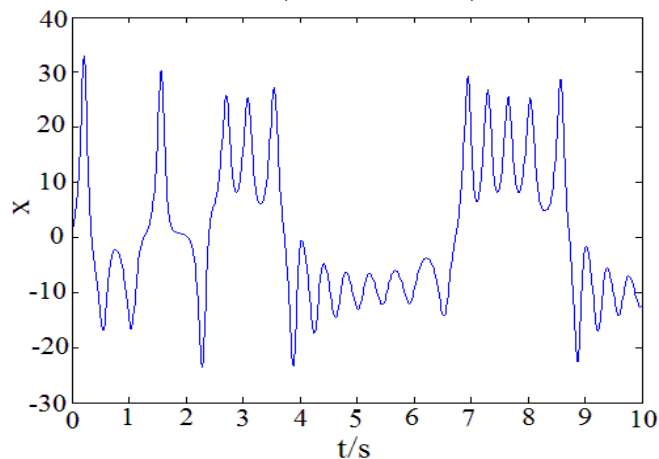
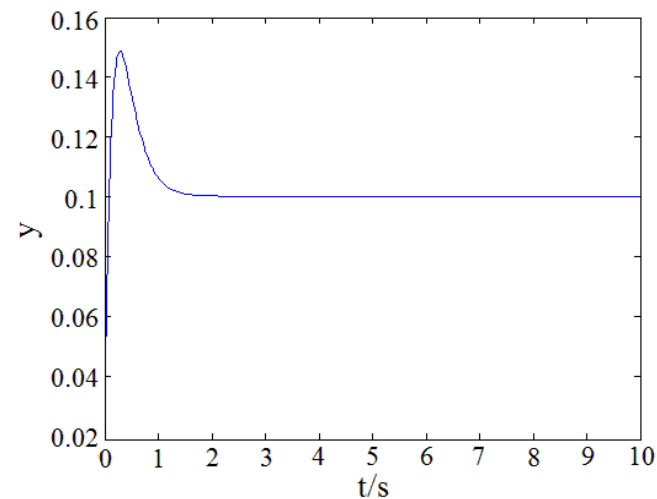
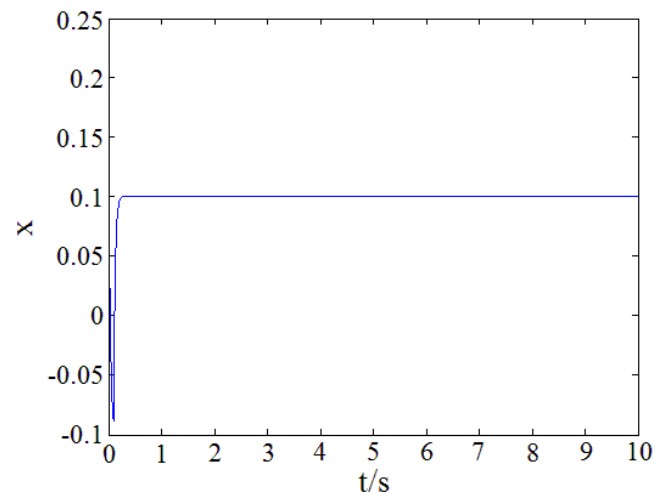
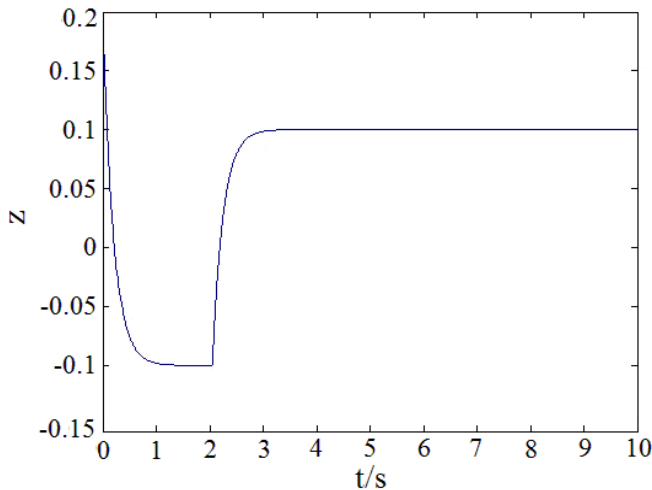


Fig. 6. Time domain charts of state variables before control.

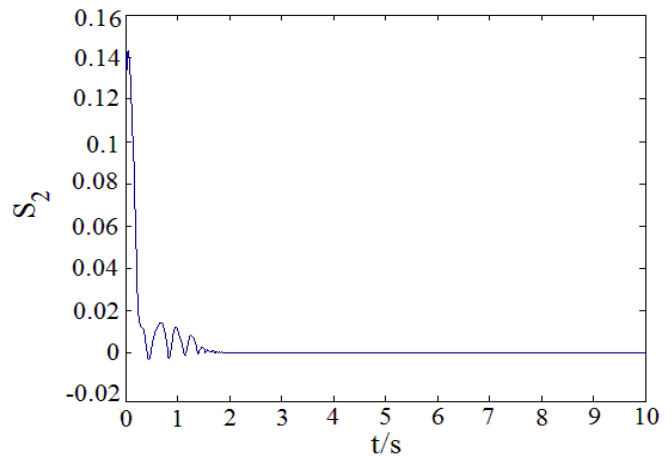
Select the proportional integral sliding mode surface as follows:

$$\begin{cases} S_1 = e_1 + \int_0^t 5e_1(\tau) d\tau, \\ S_2 = e_2 + \int_0^t 5e_2(\tau) d\tau, \\ S_3 = e_3 + \int_0^t 5e_3(\tau) d\tau, \\ S_4 = e_4 + \int_0^t 5e_4(\tau) d\tau, \end{cases} \quad (34)$$

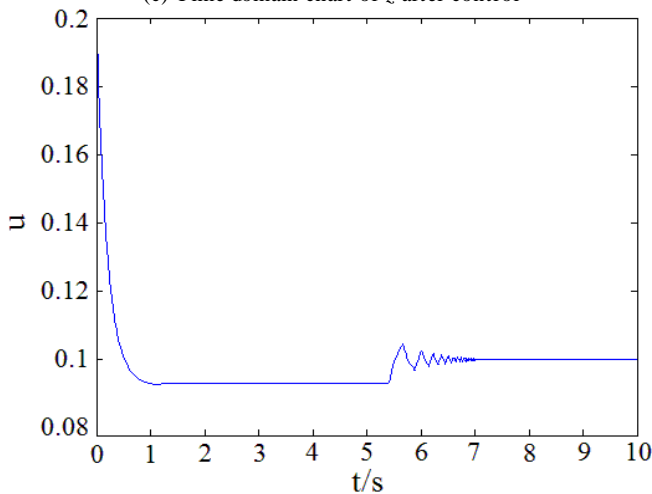




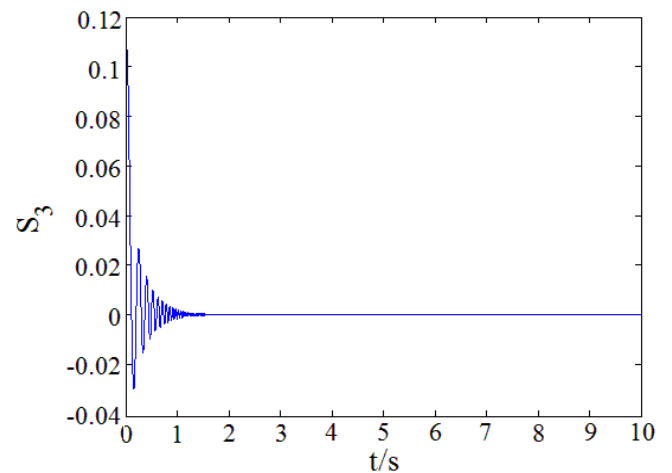
(c) Time domain chart of z after control



(b) Time domain chart of S_2 after control



(d) Time domain chart of u after control



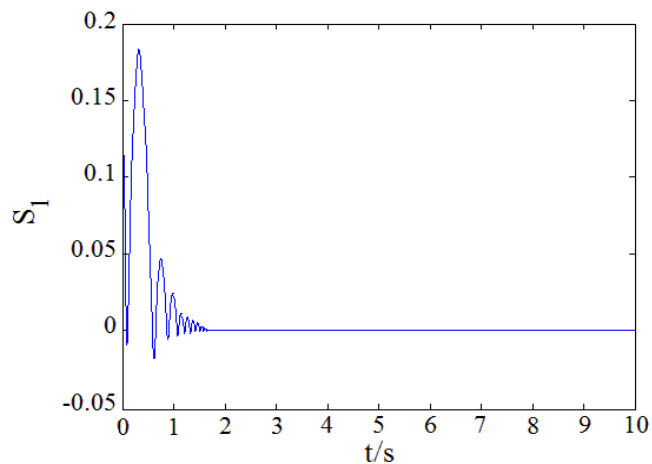
(c) Time domain chart of S_3 after control

Fig. 7. Time domain charts of state variables after control.

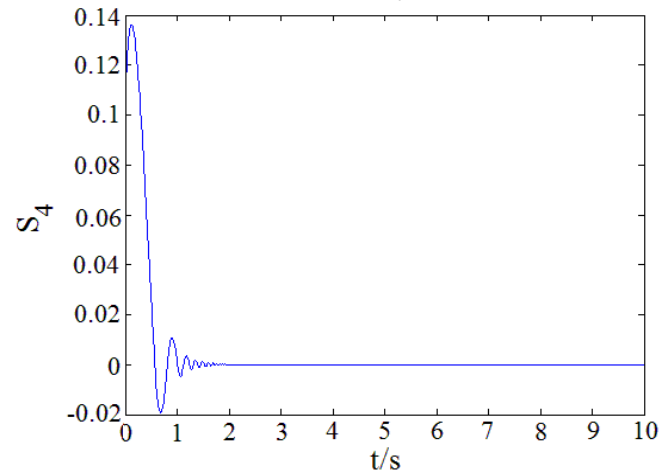
Set the initial value $[x_1(0), x_2(0), x_3(0), x_4(0)] = [0.1, 0.1, 0.1, 0.1]$, and the reference state $x_{d1} = x_{d2} = x_{d3} = x_{d4} = x_d$.

Following is the control signal

$$\begin{cases} u_1 = 15e_1 - 35e_2 - (15x_d - \dot{x}_d) - \varepsilon \text{sign}(S_1), \\ u_2 = xz - (20e_1 + 4e_2 - e_4) - (18x_d - \dot{x}_d) \\ \quad - (\varepsilon + |xz|) \text{sign}(S_2), \\ u_3 = -xy + 5e_1 - (-10x_d - \dot{x}_d) - (\varepsilon + |xy|) \text{sign}(S_3), \\ u_4 = -4e_1 - 5e_2 - (4x_d - \dot{x}_d) - \varepsilon \text{sign}(S_4). \end{cases} \quad (35)$$



(a) Time domain chart of S_1 after control



(d) Time domain chart of S_4 after control

Fig. 8. Time domain charts of sliding surfaces after control.

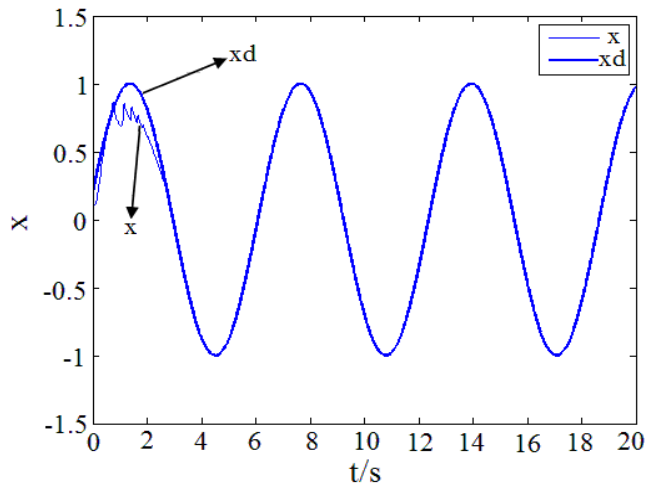
6.3 Control to the fixed point

We can stabilize the system (27), and let the system's state to reach any point by this method. In this paper, we select the fixed point $[0.1, 0.1, 0.1, 0.1]$, reference state $x_d = 0.1$, small parameter $\varepsilon = 3$ and the initial value of sliding mode surface $[S_1(0), S_2(0), S_3(0), S_4(0)] = [0.1, 0.1, 0.1, 0.1]$. We activated the controller $u(t)$ at $t = 0.1s$, and get the time domain charts of state variables and sliding surfaces as show in Fig. 7 and Fig. 8, respectively.

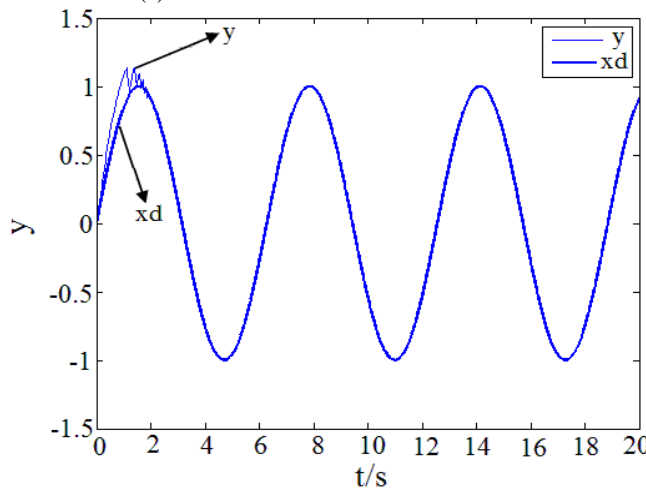
The Fig. 7 and Fig. 8 indicate that the system(27) track to the reference state $[0.1, 0.1, 0.1, 0.1]$ ultimately and the sliding mode surface S become zero after join the controller. It's proves that the system (27) reached the sliding mode.

6.4 Control to the periodic orbit

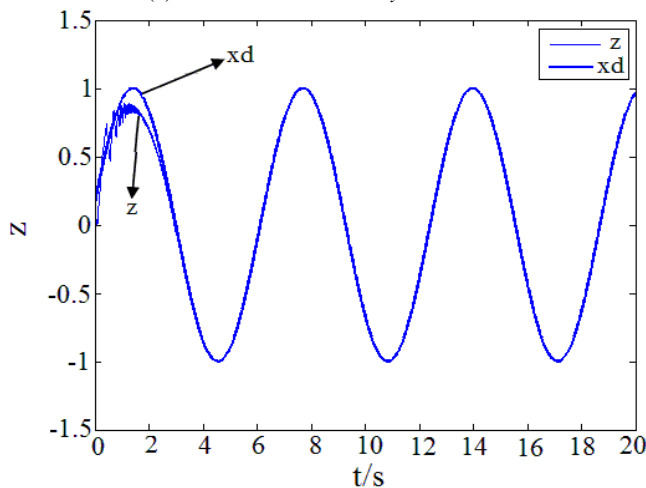
We can also stabilize the system (27), and let the system's state to reach a periodic orbit. We select the reference state $x_d = \sin(t)$. Then activated the controller $u(t)$ at $t = 1s$, and we get the time domain charts of state variables as show in Fig. 9. Obviously, the system (27) tracks to reference state $x_d = \sin(t)$ to the periodic orbit ultimately.



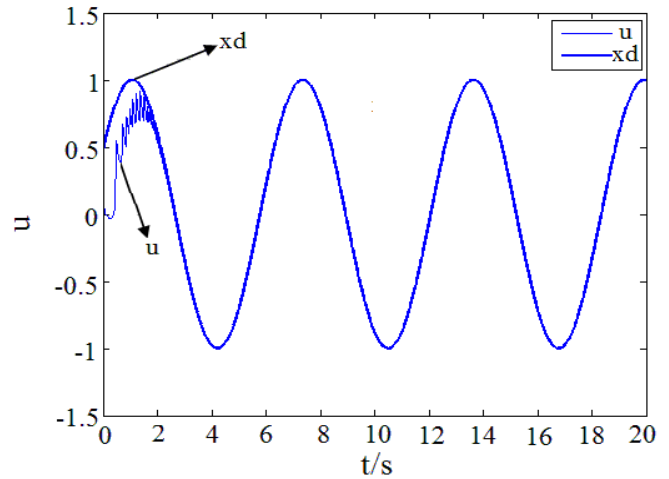
(a) Time domain chart of x after control



(b) Time domain chart of y after control



(c) Time domain chart of z after control



(d) Time domain chart of u after control

Fig. 9. Time domain charts of state variables after control.

VII. CONCLUSION

The paper investigated the basic dynamic characteristics of a new hyperchaotic system. First, the existence and local stability of the equilibrium are discussed. Then, we choose m as the bifurcation parameter and studied the existence and stability of Hopf bifurcation of the system by using the center manifold theorem and bifurcation theory. In addition, in order to eliminate the chaotic vibration, we used sliding mode method and controlled the system to any fixed point and any periodic orbit. Numerical simulation results show that the hyperchaotic system (1) occurs Hopf bifurcation when the bifurcation parameter m passes through the critical value, and the direction and stability of Hopf bifurcation can be determined by the sign of l_1 . Then the sliding mode method can make the system track target orbit strictly and smoothly with short transition time. Apparently there are more interesting problems about this chaotic system in terms of complexity, control and synchronization, which deserve further investigation.

REFERENCES

- [1] E. N. Lorenz, "Deterministic nonperiodic flow," *Journal of the atmospheric sciences*, vol. 20, no. 2, pp. 130-141, Nov. 1963.
- [2] C. Sparrow, "The Lorenz Equations: Bifurcation, Chaos, and Strange Attractors," in *Springer Science & Business Media*, first ed. vol. 41, Springer-Verlag, 175Fifth Avenue, New York, New York 10010, U.S.A, 2012, pp. 26-49.
- [3] E. Ott, "Chaos in dynamical systems," in *Cambridge university press*, 2nd ed., The Pitt Building, Trumpington Street, Cambridge, United Kingdom, 2002, pp. 115-137.
- [4] H. Li, "Dynamical analysis in a 4D hyperchaotic system," *Nonlinear Dynamics*, vol. 70, no. 2, pp. 1327-1334, Oct. 2012.
- [5] K. Zhang, Q. Yang, "Hopf bifurcation analysis in a 4D-hyperchaotic system," *Journal of Systems Science and Complexity*, vol. 23, no. 4, pp. 748-758, Aug. 2010.
- [6] X. F. Li, K. E. Chlouverakis, D. L. Xu, "Nonlinear dynamics and circuit realization of a new chaotic flow: A variant of Lorenz, Chen and Lü," *Nonlinear Analysis: Real World Applications*, vol. 10, no. 4, pp. 2357-2368, Aug. 2009.
- [7] L. F. Mello, M. Messias, D.C. Braga, "Bifurcation analysis of a new Lorenz-like chaotic system," *Chaos, Solitons & Fractals*, vol. 37, no. 4, pp. 1244-1255, Aug. 2008.
- [8] F. M. Amaral, L. F. C. Alberto, "Stability region bifurcations of nonlinear autonomous dynamical systems: Type-zero saddle-node bifurcations," *International Journal of Robust and Nonlinear*

- Control*, vol. 21, no. 6, pp. 591-612, Apr. 2011.
- [9] G. Licsko, A. Champneys, C. Hos, "Nonlinear analysis of a single stage pressure relief valve," *IAENG International Journal of Applied Mathematics*, vol. 39, no. 4, pp. 286-299, 2009.
- [10] F. S. Dias, L. F. Mello, J. G. Zhang, "Nonlinear analysis in a Lorenz-like system," *Nonlinear Analysis: Real World Applications*, vol. 11, no. 5, pp. 3491-3500, Oct. 2010.
- [11] J. Sotomayor, L. F. Mello, D. C. Braga, "Bifurcation analysis of the Watt governor system," *Computational & Applied Mathematics*, vol. 26, no. 1, pp. 19-44, 2007.
- [12] Y. A. Kuznetsov, "Elements of Applied Bifurcation Theory," in *Springer Science & Business Media*, 2nd ed. vol. 112, Springer-Verlag, New York, Berlin Heidelberg, 2013, pp. 293-390.
- [13] X. B. Zhang, H. L. Zhu, H. X. Yao, "Analysis of a new three-dimensional chaotic system," *Nonlinear Dynamics*, vol. 67, no. 1, pp. 335-343, Jan. 2012.
- [14] D. Jana, S. Chakraborty, N. Bairagi, "Stability, nonlinear oscillations and bifurcation in a delay-induced predator-prey system with harvesting," *Engineering Letters*, vol. 20, no. 3, pp. 238-246, 2012.
- [15] J. H. Lee, Paul E. Allaire, G. Tao, and X. Zhang, "Integral sliding-mode control of a magnetically suspended balance beam: analysis, simulation, and experiment," *IEEE/ASME Transactions on Mechatronics*, vol. 6, no. 3, pp. 338-346, Sep. 2001.
- [16] T. Kobayashi, S. Tsuda, "Sliding mode control of space robot for unknown target capturing," *Engineering Letters*, vol. 19, no. 2, pp. 105-111, 2011.
- [17] D. Y. Chen, Y. X. Liu, X. Y. Ma, R. F. Zhang, "No-chattering sliding mode control in a class of fractional-order chaotic systems," *Chinese Physics B*, vol. 20, no. 12, pp. 120506, Dec. 2011.
- [18] D. Y. Chen, T. Shen, X. Y. Ma, "Sliding mode control of chaotic vibrations of spinning disks with uncertain parameter under bounded disturbance," *Acta Phys. Sin.*, vol. 60, no. 5, pp. 050505, May 2011.
- [19] D. Y. Chen, P. C. Yang, X. Y. Ma, Z.T. Sun, "Chaos of hydro-turbine governing system and Its control," *Proceedings of the CSEE*, 2011, 14: 018.
- [20] Z. Z. Gao, X. F. Han, M. L. Zhang, "A novel four-dimensional hyperchaotic system and its circuit simulation," *Journal of Northeast Normal University (Natural Science Edition)*, vol. 44, no. 1, pp. 77-83, Mar. 2012.
- [21] A. Wolf, J. B. Swift, H. L. Swinney, J. A. Vastano, "Determining Lyapunov exponents from a time series," *Physica D: Nonlinear Phenomena*, vol. 16, no. 3, pp. 285-317, Jul. 1985.